LA-UR 90-3457

CONF-9010230--3

Los Alamos National Laboratory is operated by the University of California for the United States Department of Energy under contract W-7405-ENG-36

LA-UR--90-3457

DE91 002322

TITLE: CONFINEMENT PROPERTIES OF THE RFP.

AUTHOR(S): P. G. Weber, K. F. Schoenberg, J. C. Ingraham, G. Miller, C. P. Munson, M. M. Pickrell, G. A. Wurden, H. Y. W. Tsui, Ch. P. Ritz and R. F. Ellis.

SUBMITTED TO: International School of Plasma Physics, Varenna, Italy, Oct 14-24, 1990.

DISCLAIMER

Los Alamos National Laboratory
Los Alamos, New Mexico 87545

FORM NO. 836 R4
ST. NO. 2629 5/81

CONFINEMENT PROPERTIES OF THE RFP. [1]

P. G. Weber, K. F. Schoenberg, J. C. Ingraham, G. Miller,
C. P. Munson, M. M. Pickrell and G. A. Wurden
Los Alamos National Laboratory, Los Alamos, NM 87545, USA.

H. Y. W. Tsui and Ch. P. Ritz
Fusion Research Center, University of Texas, Austin, TX 78712, USA.

R. F. Ellis
University of Maryland, College Park, MD 20742, USA.

Abstract

Research in ZT-40M has been focused on elucidating the confinement properties of the Reversed Field Pinch (RFP). Recent improvements in diagnostic capability have permitted measurement of radial profiles, as well as a detailed study of the edge plasma.

The emerging confinement picture for ZT-40M has several ingredients:
• Typically 0.3 of the Ohmic input power to ZT-40M is available to drive fluctuations. Evidence points to this fluctuational power heating the ions.
• Approximately one quarter of the input power is lost through radiation, with metal impurities playing a key role.
• Magnetic fluctuations in ZT-40M are at the percent level, as measured in the edge plasma. Extrapolating these data to small radii shows stochasticity in the core plasma.
• Suprathermal electrons ($T_{supra} \sim 2-3 \times T_e(0)$) are measured in the edge plasma. These electrons originate in the core, and transport to the edge along the fluctuating magnetic field lines. Under typical conditions, these electrons constitute the major electron energy loss channel in ZT-40M.
• Electrostatic fluctuations dominate the edge electron particle flux, but not the electron thermal flux.
• The major ion loss process is charge exchange, with smaller contributions from conduction and convection.

In examining these observations, and the parametric dependences of confinement, a working model for RFP confinement emerges. An overview of this model, together with implications for the multi-mega-ampere ZTH experiment will be presented.

[1] Work performed under the auspices of the U. S. Department of Energy

INTRODUCTION.

It is well-known that the energy loss rate from toroidal magnetic confinement devices is much larger than predicted by (neo-)classical theory [1,2]. A major goal of magnetic confinement fusion research is therefore to understand and improve (as necessary) the plasma energy confinement. It is generally thought that the anomalously poor confinement is the result of plasma instabilities generating turbulence with associated higher loss rates.

Such turbulent transport may be divided into two components: electrostatic and magnetic. Electrostatic transport is a result of the correlation between plasma pressure fluctuations and the fluctuating radial electrostatic drift given by $\tilde{\mathbf{E}} \times < \mathbf{B} >$ where the $\tilde{\mathbf{E}}$ is driven by the turbulence. Magnetic turbulence is the result of magnetic flutter breaking up flux surfaces, leading to increased transport.

The driving forces for the $\tilde{\mathbf{E}}$ and $\tilde{\mathbf{B}}$ include the magnetic field structure, pressure gradients, resistivity gradients, impurity distributions, trapped particles, current relative to the magnetic field, etc.[3].

In principle, one wishes to identify the physical mechanisms underlying the losses from the plasma, relate them to a complete theory, and take the steps required to ameliorate any problems. In practice, many processes are active simultaneously in various regions of the plasma, and available diagnostics are unable, for example, to measure the full fluctuation spectra as functions of position, wavelength, frequency, time and plasma conditions. Similarly, theories often deal with only a single instability or drive mechanism, and use simplifying assumptions to arrive at a solution to a very complicated problem.

Thus, in practice, the experimentalist measures as many relevant quantities as possible [4,5] within technological and resource limitations and attempts to relate the observations to pertinent theoretical work. Similarly, theories can be tested by documenting the relevant measurable parametric dependences and looking for characteristic signatures. Even the resulting limited understanding can form a guide to the next logical step in the sequence leading to an eventual reactor.

This paper follows the latter, rather practically oriented procedure. The present

paper concentrates on ZT-40M[6] data, although similar information may be available from elsewhere [7 and references there-in]. Recent work on the ZT-40M RFP has included measurements of profiles of plasma temperatures, densities, radiated power [8], and magnetic fields [9]. Furthermore, detailed studies of the edge plasma, using a variety of probes, has been used to make estimates of the electrostatic [10] and magnetic [11] turbulence and transport consequences [12,13]. These data are combined to form a working model for the transport processes in ZT-40M, and are extended to predict the important transport mechanisms in the multi-mega-ampere RFX and ZTH [14] experiments now under construction.

POWER INPUT TO ZT-40M.

The Reversed Field Pinch power input is given by: $P_{in} = I_\phi V_\phi - I_\theta V_\theta$ (the second term is typically sufficiently small to be neglected). Thus P_{in} is readily measured by voltage loops and Rogowski coils. Auxiliary heating is not used in the RFP, and is projected not to be necessary for a reactor [15].

Within the context of MHD, one can quantitatively estimate the fraction (P_F) of this input power directly absorbed by fluctuations in the discharge[16]. Following the referenced paper[16], one computes an effective resistivity from energy balance:

$$dW/dt = I_\phi V_\phi - I_\theta V_\theta - \int \mathbf{E} \bullet \mathbf{J}\, dV,$$

where W is the energy, I_x denotes current, V_x denotes voltage, $\mathbf{E}$ is the electric field vector and $\mathbf{J}$ is the current density. Substituting in terms of the parallel and perpendicular components of resistivities and current density, and in terms of the steady state and fluctuating components, one obtains:

$$dW/dt = I_\phi V_\phi - I_\theta V_\theta - \int \eta_{||}(< J_{||} >^2 + < \tilde{J}_{||}^2 >) + \eta_\perp < \tilde{J}_\perp^2 > - < \mathbf{v} \times \mathbf{B} \bullet \mathbf{J} > dV.$$

One now defines an effective ("energy balance") resistivity, η^W, from

$$dW/dt = I_\phi V_\phi - I_\theta V_\theta - \int \eta_{||}^W < J_{||} >^2 dV.$$

The fluctuational power absorption is then given by:

$$\int \eta_{||} < \tilde{J}_{||}^2 > + \eta_\perp < \tilde{J}_\perp^2 > - < \mathbf{v} \times \mathbf{B} \bullet \mathbf{J} > dV = \int (\eta_{||}^W - \eta_{||}) < J >^2 dV$$

Similarly, one defines helicity balance from:

$dK/dt = 2\Phi V_\phi - 2\int \mathbf{E} \bullet \mathbf{B} dV,$

where $K \equiv \int \mathbf{A} \bullet \mathbf{B} dV$ is the magnetic helicity.

Following a similar procedure to the above, one defines an effective "helicity balance" resistivity η^K from:

$dK/dt = 2\Phi V_\phi - 2\int \eta_{||}^K < \mathbf{J} > \bullet < \mathbf{B} > dV.$

The fluctuational helicity absorption is then given by:

$\int \eta_{||} < \tilde{\mathbf{J}} \bullet \tilde{\mathbf{B}} > dV = \int (\eta_{||}^K - \eta_{||}) < \mathbf{J} > \bullet < \mathbf{B} > dV$

The effecive resistivities η^K and η^W differ mostly in that the η^W contains all of the $\mathbf{v} \times \mathbf{B}$ fluctuational power. Thus, one obtains for the operating regimes of the RFP: $P_F = 1 - \eta^K/\eta^W$ to be the fraction of the Ohmic input power absorbed by fluctuations. This result is insensitive to reasonable resistivity profiles, and that it is independent of Z_{eff}.

For typical ZT-40M conditions, (120 kA, $\Theta = 1.45$, $n_e \sim 1 - 2 \times 10^{19} m^{-3}$) P_F is roughly 0.3. P_F is strongly correlated with ion heating [17]; for example, with $P_F \simeq 0.3$ one sees $T_e \simeq T_i$, while for an extreme case with $P_F \simeq 0.4$ to 0.5, one can observe $T_i \sim 1 keV$ with $T_e(0) \sim 300 eV$ [18]. This strong correlation suggests a fluctuation driven ion heating mechanism [19].

Thus, for typical ZT-40M conditions, 0.3 of the input power goes into fluctuations, and thence into ion heating (Fig. 1). (Note in passing that the fluctuations can also cause Eddy current dissipation in the wall, and furthermore that wave-particle interactions may couple some fluctuational power to the electrons. These powers are assumed to be small.) One then has some 0.7 of the input power being dissipated in Ohmically heating the electrons.

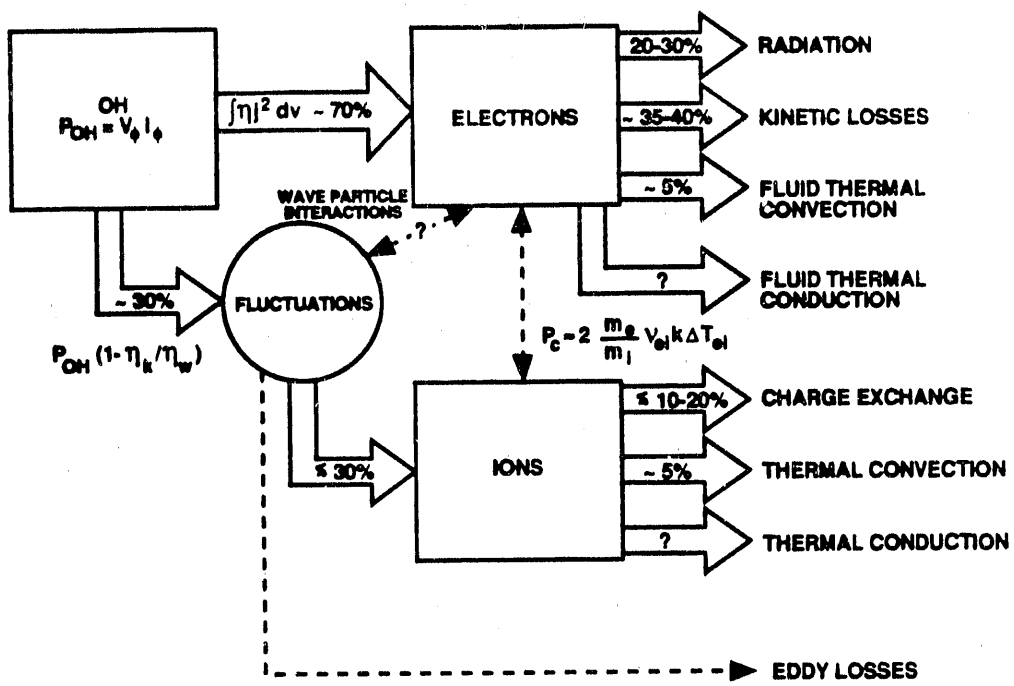

Fig. 1.: Global power flow diagram for 120 kA ZT-40M discharges.

The collisional equipartition of energy between the electrons and ions takes place on a timescale several times longer than the energy confinement time, even if the ion temperature were very much less than the electron temperature. Since the fluctuational ion heating in ZT-40M typically gives comparable T_i and T_e, the energy transfer between electrons and ions is typically small.

PROFILE MEASUREMENTS.

Very limited profile data is routinely available from present RFP experiments. For example, multi-point Thomson scattering has been available only on $\eta\beta II$ [20] and on ZT-40M [21]. Consequently, global confinement parameters are usually based on the central temperature and line average density measurements sometimes coupled with assumed profile corrections. Similarly, there is little data documenting pressure gradients which may drive instabilities [3].

ZT-40M has some arrays in routine operation [5]. There are eight surface barrier diodes in one poloidal cross-section [22], as well as six spectrometers [23,24]. These instruments provide qualitative information on impurities and electron temperature profiles. An eight chord bolometer array [8] routinely provides the radiated power profile, and eight Balmer-alpha spectral line monitors give the Deuterium recycling rate[24]. Magnetic field radial profiles have been measured at low currents [9], and are well-approximated by the modified Bessel function model (MBFM) with $\mu(r) \equiv j(r)/B(r)$ adjusted to fit the fields and fluxes determined in the edge. Some recent insights have been gained on ZT-40M, both from multipoint Thomson scattering and from moving the location of some diagnostics on a shot-to-shot basis.

For the present exercise, the single point Thomson scattering diagnostic was operated at radii of 0, 14.5 and 16.3 cms, the two-chord FIR interferometer [25] at (0, 12.6) and (4.2, 16.8) cm impact parameters, and the CV Doppler broadening spectrometer [26] was used at radii from -12.6 to +16.8 cms in 4.2 cm increments. The data were entered into a Locus database [27] together with dozens of other pieces of diagnostic data. This permitted a selection of shots with very comparable parameters from several runs.

As an early example of the results, Fig. 2 shows the ratio of the line average density at 16.8 cms impact parameter("n_{16}") to that at 4.2 cms ("n_4") for plasma currents from about 80 to 170 kA. The data are obtained at 5 ms into the discharge, where the current has already been time-invariant for several ms; the data are sorted into bins by the current level and plotted as averages with error bars denoting the standard deviations. No density control is attempted in these runs; rather, the density is a result of the fill pressure and wall conditioning and is, at 5 ms, changing only slowly in time. It is immediately clear that the electron density profile is rather narrow at the lowest currents, but becomes broader as plasma current is increased.

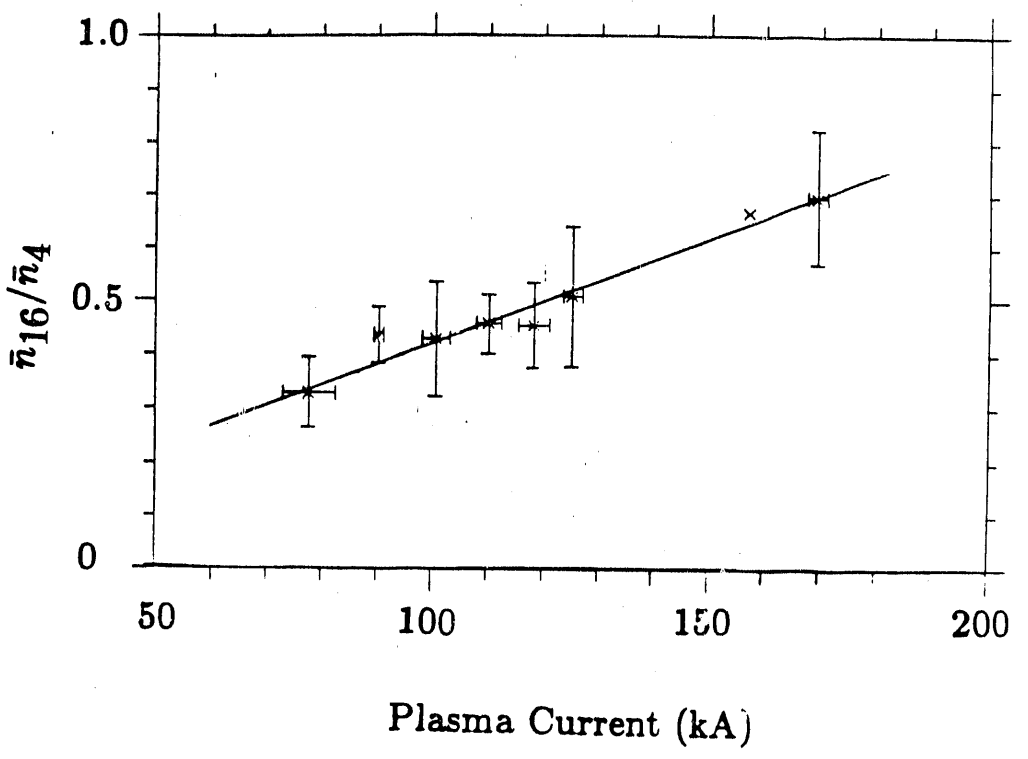

Fig. 2.: Ratio of densities on chords at 16.8 and at 4.2 cm impact parameter as a function of plasma current showing density profile broadening with plasma current in the absence of density control.

Single point Thomson scattering data at the 16.3 cm radius is subject to larger uncertainties than at other locations due to the heavily vignetted collection optics. Electron temperature profiles at 120 kA can be fitted to the form $T_e(r) = T_e(0)[1 - (r/a)^n]$ where the index n is nominally five, but subject to a large uncertainty. Spectroscopic measurements at 120 kA show that CV still emits at the 16.8 cm impact parameter consistent with the 100 eV electron temperature found at r=16.3 cms by Thomson scattering. The Doppler broadening ion temperature at this impact parameter was also about 100 eV, compared to 130 $\pm$ 30 eV at the diameter chord, indicating a quite flat $T_i(r)$. The profile is broader than the quartic Deuterium ion temperature profile ascertained from neutral particle analyzer data [28], although the plasma conditions were different for the NPA data.

Given these data, one can compute the true plasma pressure and confinement

times. When computing the total plasma pressure one is particularly sensitive to the contributions from the plasma edge (due to the large volume represented by the edge plasma). The data in the edge have the largest uncertainties. Thus errors in computed β and confinement time τ are large, covering about a factor three from the lowest to the highest values consistent with the data. Figure 3 shows these ranges for three plasma conditions: 120 kA with the normal line average density of $1.5 \times 10^{19} m^{-3}$, 180 kA with a higher than normal density of $3 \times 10^{19} m^{-3}$ and shots at 170 kA with a diameter average density of $4 \times 10^{19} m^{-3}$ and Krypton impurities added to increase the radiated power to eighty percent of the Ohmic input power. Operationally, one claims a fairly constant range of poloidal beta over these various conditions.

In terms of pressure gradients, one is again faced with the fact that data in the edge are very limited. Typically, one sees small gradients in the core, with most of the pressure gradient in the edge. This is consistent with magnetic fluctuation data (see below), which indicate stochasticity in the core with superior confinement at $r > \frac{2}{3}a$.

LOSS PROCESSES.

Loss processes have been quantified in ZT-40M using a variety of diagnostics. Radiative losses are measured using a spatially resolving array of bolometers [8]. For typical ZT-40M conditions (e.g. $I_\phi = 120kA, n_e = 1 - 2 \times 10^{19} m^{-3}$) one sees 0.2 to 0.3 of the input power being radiated. The bolometers have been tested for possible effects of particles impinging on the foil; such effects are small for normal 120 kA discharges. Metal impurities are responsible for most of the radiated power and contribute strongly to Z_{eff} [24].

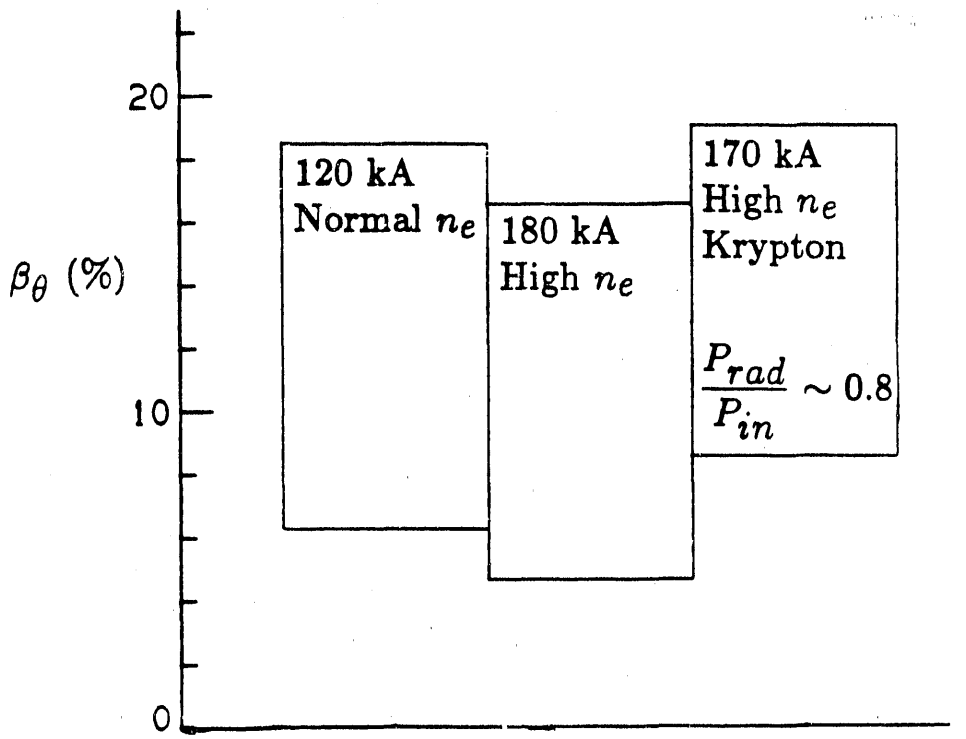

Fig. 3.: Total plasma beta computed for three plasma conditions with best profile information included. Vertical size of boxes indicates the uncertainty in the data.

The subject of magnetic fluctuations and the concommitant leakage of suprathermal electrons are discussed in detail elsewhere in these proceedings (Miller and Ingraham); a short summary is given here. Magnetic fluctuations at the percent level are measured in the edge plasma. Using quasi-static eigenfunctions, one can extrapolate the fluctuation level into the core plasma [29]. One observes strong m=1 modes with n numbers such as to be resonant with the magnetic field pitch in the core. These modes correspond to those seen in 3-D M.D computations [29], and have been identified as a possible driver for magnetic field profile maintenance [31]. The fluctuation levels found experimentally are, however, much smaller than those predicted by the simulations. At higher (m,n), modes are observed with higher powers than predicted by the zero-pressure 3-D MHD computations. These modes are resonant with the magnetic field in the exterior regions of the plasma, where pressure gradients are found. This indicates that pressure driven modes

may exist in ZT-40M. In summary, one sees magnetic fluctuations at roughly the percent level throughout the ZT-40M plasma.

These fluctuations act to increase the loss rate of particles from the plasma core. A useful model for this increased transport is found in the electron thermal conduction theory of Rechester and Rosenbluth [32]. In this model, electrons are accelerated by the applied parallel electric field ($E_{||} = \mathbf{E} \bullet \mathbf{B}/B$) in the core region of the discharge. Magnetic fluctuations then facilitate the transport of (especially) energetic electrons across radius. Within the context of this model, the electrons will maintain their directed velocity over a radial extent $\Delta r \simeq (2\lambda D_F)^{0.5}$ where $D_F = (\tilde{B}_r/B)^2 l_c$ is the magnetic diffusivity, λ is the electron mean free path and l_c is the correlation length. The dependence of mean free path λ on electron speed v: $\lambda \ \alpha \ v^4$ enables faster electrons to traverse most of the plasma radius without losing the velocity $v_{||}$ attained in the core. As an example, for the magnetic fluctuations in ZT-40M, the radial step size Δr is about the minor radius, a, for electrons traveling at twice the thermal speed in the core [33].

Indeed, such suprathermal electrons are measured in the ZT-40M edge plasma using an electron energy analyzer. Details of these measurements are presented elsewhere in these proceedings (Ingraham) and in Refs. 34 and 35; a short summary follows. The bulk edge plasma has electron temperatures of 10-40 eV, and densities of order twenty percent of the core density. These conditions are similar to those found in other toroidal magnetic confinement devices, such as the tokamak and stellarator. In ZT-40M one also measures a small population (less than ten percent of the *edge* density) of electrons with effective temperatures $T_{supra} \sim 2 - 3 \times T_e(0)$, moving almost unidirectionally along the local magnetic field. While the density of these suprathermal electrons is small, their influence in the discharge is large. Specifically, the suprathermal electron heat flux typically comprises 0.35-0.4 of the ZT-40M input power; this is denoted as "kinetic losses" in the power flow diagram (Fig. 1.). Furthermore, the suprathermal electrons can carry most of the parallel current density in the exterior of the plasma ($r/a > 0.7$), thus providing a mechanism for maintaining the reversed toroidal magnetic field configuration [34]. Since the suprathermals move almost unidirectionally along the magnetic field lines, and carry a large power flux (450 MW/m^2), they are

responsible for most of the energy asymmetry observed in the RFP edge plasma. Finally, since the suprathermals transport momentum to the wall, they can increase the loop voltage in the RFP [36].

Next, consider the increased transport rate caused by *electrostatic* fluctuations. An array of Langmuir probes in the edge plasma is used to ascertain the relevant parameters n, T, ϕ, E, v and their fluctuating parts $\tilde{n}, \tilde{T}, \tilde{\phi}, \tilde{E}, \tilde{v}$ [10]. The quadratic combinations of these quantities yield net transport. For example [37], the particle flux driven by electrostatic fluctuations is given by $\Gamma_E =< \tilde{n}\tilde{v}_r > = - < \tilde{n}\nabla\tilde{\phi} > /B$ where $\tilde{v}_r$ is the radial fluctuating velocity driven by the fluctuating local electric field $\tilde{E} = -\nabla\tilde{\phi}_p$; in ZT-40M, this flux is roughly equal to the total edge particle flux measured spectroscopically [24]. Thus, as in a tokamak, electrostatic turbulence is identified as an important edge *particle* transport mechanism.

The electrostatically driven heat flux Q_E may be described in terms of a conductive and a convective component: $Q_E = Q_{cond} + Q_{conv}$ where $Q_{cond} \equiv \frac{3}{2}nk < \tilde{T}\tilde{v}_r >$, and $Q_{conv} = \frac{3}{2}kT < \tilde{n}\tilde{v}_r >$. In ZT-40M Q_{cond} and Q_{conv} are both small ($\sim$ 5 percent) compared with the total heat flux [13]. This is consistent with the hypothesis that $\tilde{B}$ transport dominates energy confinement in present RFPs and contrasts with observations in tokamaks and stellarators where Q_E contributes strongly to the total edge *thermal* flux [38, 39]. Another observation is that $\tilde{T}$ and $\tilde{n}$ are anti-correlated, which implies Q_{cond} is directed inward [10].

In ZT-40M: $\tilde{n}/n \sim 0.3$ -- $0.5 < \tilde{\phi}_{fl}/kT_e \sim 1$, as also seen in a tokamak [38] and in models that involve the effects of radiation on edge turbulence. Further work is required in this area; data from highly radiating plasmas [40] will be especially instructive in this regard.

Similarly, ion losses by electrostatic fluctuations in the edge are small.

Ion losses from charge exchange are estimated from the particle flux observed with the time-of-flight neutral particle analyzer ("TOF") [41]. These losses are estimated to be in the range ten to twenty percent of the Ohmic input power to ZT-40M.

One now adds up the measured losses, and finds that the total identified losses are

in the range of 75-100 percent of the input power. This uncertainty is indicated in Fig. 1. by arrows indicating "other losses" of $\leq 10\%$ for the electrons and $\leq 15\%$ for the ions.

Thus Fig. 1. is a reasonable zero order picture of the power flows in ZT-40M. The relatively large magnetic fluctuations allow a leakage of suprathermal electrons from the core to the edge. This is the major electron energy loss process in ZT-40M. Radiation is another strong loss mechanism, (mostly attributed to metal impurities), while electrostatic fluctuations do not contribute much to energy losses (although they are important in edge *particle* losses). The ions are heated anomalously, and their major loss channel is through charge exchange.

IMPLICATIONS FOR NEXT GENERATION RFPs.

Let us now investigate the implication of the ZT-40M power flow and confinement measurements for the multi-mega-ampere ZTH experiment. (Similar extrapolations could be made to RFX, which differs from ZTH in several aspects, including the magnetic boundary conditions and the shell time constant.) The present extrapolation is based on examining the variations observed in the measurable quantities as a function of dimensionless parameters; the hope being that one may elucidate some underlying physics in this process. As an example, let us examine (Fig. 4) the dependence of the magnetic fluctuations observed on flux loops as a function of the Lundquist number, S. These flux loops are external to the vacuum liner, thus restricting our observations to relatively low frequencies. The *rms* amplitude of these fluctuations decreases as $S^{-0.4\pm0.1}$. Without detailed radial profile data on these fluctuations, it is difficult to associate this scaling with a particular model or instability. However, as an example, the turbulence associated with electrostatic resistive g-modes, which are resonant outside the core should give $\tilde{B}_r \propto S^{-0.5}$ with constant electron beta [42, 43], in reasonable agreement with the present experimental data.

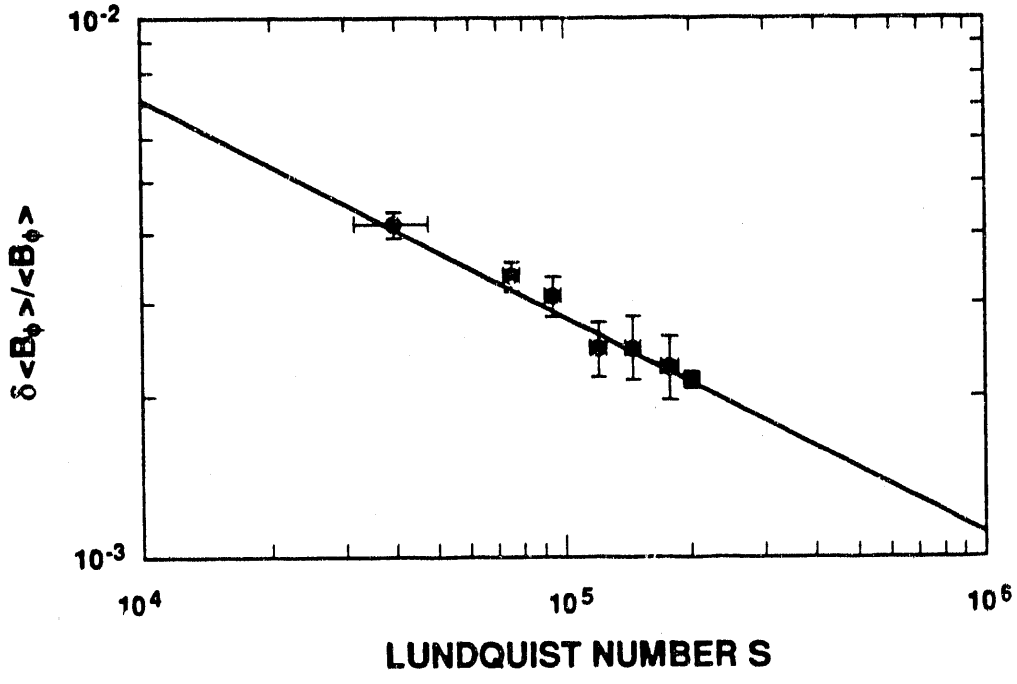

Fig. 4.: Dependence of fluctuation amplitude observed on flux loops outside the vacuum liner on the Lundquist number, S. The fitted line has a slope of -0.4 ± 0.1.

Preliminary modeling of the suprathermal electron transport by solving the long mean free path (collisionless) limit of the Boltzmann equation, assuming magnetic flutter driven transport, yields qualitative agreement between the calculated and measured electron distribution function, the magnitude of the magnetic field flutter, and the applied electric field E_ϕ [44]. As an example, one can estimate the additional resistivity of the plasma due to momentum transfer to the wall as [36]: $\eta_K/\eta_{Spitzer} \simeq [1 + (\kappa P/\Theta)(E_\phi/E_R)]$ where $\kappa \sim 2.5$, η_K is the helicity balance resistivity, P is the power deposition asymmetry factor on the wall, $\Theta \equiv B_\theta(a)/ < B_\phi >$, E_ϕ is the applied electric field and E_R is the critical field for run-away. A plot of ZT-40M data (Fig. 5) shows a similar dependence, although the ratio $\eta_K/\eta_{Spitzer}$ here also includes contributions from impurities.

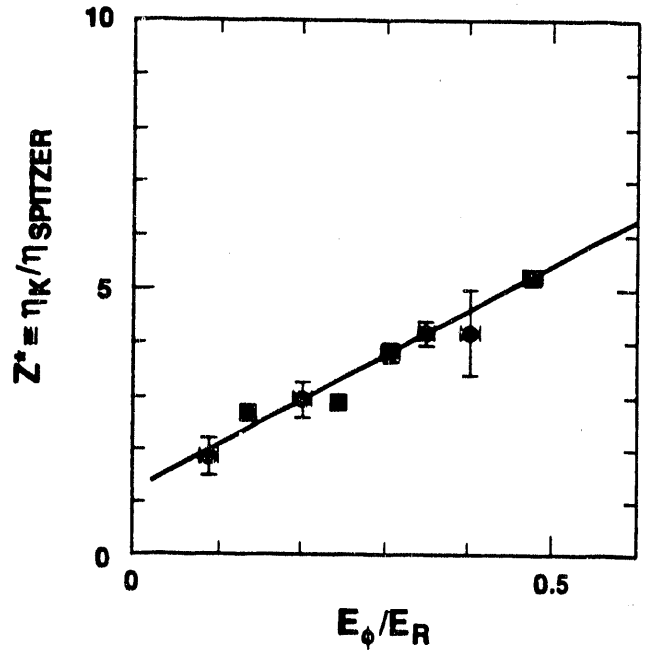

Fig. 5.: Plasma resistive anomaly factor (ratio between the resistivity determined from helicity balance and Spitzer value based on Thomson scattering) as a function of the electric field relative to the critical field for run-away.

Thus, by increasing the Lundquist number S the magnetic fluctuations should be diminished, reducing the magnetic stochasticity. By further designing an experiment to have minimal magnetic field errors at the boundary, one reduces excitation of modes resonant with those applied externally. By reducing the electron acceleration, i.e. by reducing E_ϕ/E_R one reduces the deleterious effects of suprathermal electron transport on plasma resistivity.

ZTH is designed to move precisely in these directions. Present RFPs operate in a narrow range of poloidal beta, and with temperatures increasing with plasma current [6]. Assuming that ZTH will maintain these characteristics, which leads to a factor 100 increase in the Lundquist number for ZTH at 2 MA relative to typical ZT-40M operation. Assuming magnetic fluctuations continue to decrease as the square root of S leads to a large decrease in the expected level of these

fluctuations in ZTH. Furthermore, ZTH is designed [45] to have much improved magnetic boundary conditions. The 48 toroidal magnetic field coils are removed significantly from the plasma, reducing ripple. The device has an overlapping poloidal gap in the conducting shell to reduce field errors from that source [46]. The coil set is designed to have the last closed plasma flux surface coincident with the vacuum vessel to a high tolerance. Diagnostic access and pumping ports are relatively small to reduce field errors from interruptions in the liner.

ZTH has an electrically "thin" shell, meaning that the shell time constant for vertical field penetration ($\sim$ 60 ms) is short compared to the discharge duration. Therefore the equilibrium position of the plasma can be dynamically controlled with excellent precision at the shell gap (as in ZT-40M), but also globally. Experience with present RFPs points to improved confinement with improved equilibrium control.

The ZTH design operating point also gives a factor five reduction in E_ϕ/E_R relative to typical ZT-40M operation. Combined with the reduction in magnetic fluctuations, this should lead to a reduction in the kinetic electron losses.

Finally, more than 90 percent of the ZTH vacuum liner will be covered by graphite tiles [47]. Thus, assuming successful clean-up of oxygen by discharge cleaning, carbon should be the major impurity. This should lead to low radiated power fractions, and a relatively low Z_{eff}.

The combination of these ZTH design features, plus suitable diagnostics, should allow a study of the intrinsic confinement of the RFP, and permit a better evaluation of the RFP as a viable alternative confinement scheme.

REFERENCES.

[1] R. K. LINFORD, S. LUCKHARDT, J. F. LYON, G. A. NAVRATIL and K. F. SCHOENBERG, *Comments Plasma Phys. Contr. Fusion*, **13**, 311 (1990).

[2] P. C. LIEWER, *Nuc. Fusion*, **25**, 543 (1985).

[3] G. BATEMAN, *MHD Instabilities*, The MIT Press, Cambridge, MA. (1978).

[4] D. V. ORLINSKIJ and G. MAGYAR, *Nucl. Fusion*, **28**, 611 (1988).

[5] P. G. WEBER, in *Basic and Advanced Diagnostic Techniques for Fusion Plasmas*, P. E. STOTT, *et al*, Editors, CEC publishers, **III**, 941 (1987).

[6] R. S. MASSEY, R. G. WATT, P. G. WEBER, *et al*, *Fusion Technol.*, **8**, 1571 (1985).

[7] H. A. B. BODIN, *Nucl. Energy*, **29**, 57 (1990).

[8] G. MILLER, J. C. INGRAHAM and L. S. SHRANK, *Rev. Sci. Instrum.*, **59**, 700 (1988).

[9] R. B. HOWELL, J. C. INGRAHAM, L. C. BURKHARDT, E. J. NILLES and Z. YOSHIDA, *Bull. Am. Phys. Soc.*, **31**, 1547 (1986).

[10] H. Y. W. TSUI, Ch. P. RITZ, G. MILLER, *et al*, manuscript in preparation (1990).

[11] G. MILLER, J. C. INGRAHAM, C. P. MUNSON, K. F. SCHOENBERG, and P. G. WEBER, *Proc. 17th European Conf. on Contr. Fusion and Plasma Physics, Amsterdam 1990*, **14B, II**, 581 (1990).

[12] K. F. SCHOENBERG, J. C. INGRAHAM, R. W. MOSES, Jr., *et al*, *Proc 12th Int. Conf. Plasma Physics Contr. Nuclear Fusion Res., Nice 1988*, IAEA Vienna, **II**, 419 (1988).

[13] P. G. WEBER, K. F. SCHOENBERG, J. C. INGRAHAM, *et al*, *Proc. 13th Int. Conf. Plasma Physics Contr. Nuclear Fusion Res., Washington, DC 1990.* IAEA Vienna (to be published).

[14] P. THULLEN, these proceedings.

[15] H. A. B. BODIN, R. A. KRAKOWSKI and S. ORTOLANI, *Fusion Technol.*, **10**, 307 (1986).

[16] K. F. SCHOENBERG, R. W. MOSES and R. L. HAGENSON, *Phys. Fluids*, **27**, 1671 (1984).

[17] P. G. WEBER, *Bull. Am. Phys. Soc.*, **33**, 1942 (1988).

[WWS89] G. A. WURDEN, K. F. SCHOENBERG, M. M. PICKRELL, *et al*, in *Physics of Mirrors, Reversed Field Pinches and Compact Tori*, S. ORTOLANI and E. SINDONI, editors, Editrice Compositori, publishers, **I**, 159 (1988).

[19] R. W. MOSES, Jr., *Bull. Am. Phys. Soc.*, **33**, 1942 (1988).

[20] V. ANTONI, M. BAGATIN, E. BASSAN, *et al*, *Proc. 17th European Conf. on Contr. Fusion and Plasma Physics, Amsterdam 1990*, **14B, II**, 553 (1990).

[21] M. M. PICKRELL, A. GIGER, W. A. REASS, *et al*, *Bull. Am. Phys. Soc.*, **31**, 1547 (1986).

[22] G. A. WURDEN, *Phys. Fluids*, **27**, 551 (1984).

[23] R. G. WATT, Los Alamos National Laboratory Report LA-9374-MS (1982).

[24] P. G. WEBER, *Phys. Fluids*, **28**, 3136 (1985).

[25] R. M. ERICKSON, F. C. JAHODA and P. R. FORMAN, *Rev. Sci. Instrum.*, **56**, 939 (1985).

[26] R. B. HOWELL and Y. NAGAYAMA, *Phys. Fluids*, **28**, 743 (1985).

[27] J. A. MURPHY and R. M. WIELAND, *Rev. Sci. Instrum.* **59**, 1780 (1988).

[28] G. A. WURDEN, P. G. WEBER, K. F. SCHOENBERG, *et al*, *Proc. 16th European Conf. Contr. Fusion and Plasma Physics, Dubrovnik (Cavtat) Yugoslavia* (1988).

[29] G. MILLER, *Phys. Fluids*, **28**, 560 (1985).

[29] R. A. NEBEL, these proceedings.

[31] E. J. CARAMANA, R. A. NEBEL and D. D. SCHNACK, *Phys. Fluids*, **26**, 1305 (1983).

[32] A. B. RECHESTER and M. N. ROSENBLUTH, *Phys. Rev. Lett.* **40**, 38 (1978).

[33] A. R. JACOBSON and R. W. MOSES, *Phys. Rev. A.*, **29**, 3335 (1984).

[34] J. C. INGRAHAM, R. F. ELLIS, J. N. DOWNING, *et al*, *Bull. Am. Phys. Soc.*, **34**, 2105 (1989).

[35] J. C. INGRAHAM, R. F. ELLIS, J. N. DOWNING, C. P. MUNSON, P. G. WEBER and G. A. WURDEN, *Phys. Fluids*, **B2**, 143 (1990).

[36] R. W. MOSES, K. F. SCHOENBERG and D. A. BAKER, *Phys. Fluids*, **31**, 3152 (1988).

[37] See, e.g. A. WOOTTON, Fusion Research Center Report 340, Univ. Texas, (1990).

[38] Ch. P. RITZ, R. V. BRAVENEC, P. M. SCHOCH, *et al*, *Phys. Rev. Lett.*, **62**, 1844 (1989).

[39] T. UCKAN, C. HIDALGO, J. D. BELL, *et al*, *Proc. IEEE Int. Conf. Plasma Science*, IEEE90CH2857-1, 79 (1990).

[40] M. M. PICKRELL, J. A. PHILLIPS, G. MILLER, *et al Proc. 16th European Conf. Contr. Fusion and Plasma Physics, Venice Italy*, (1989).

[41] C. P. MUNSON, *Bull. Am. Phys. Soc.*, **30**, 1404 (1985).

[42] J. W. CONNOR and J. B. TAYLOR, *Phys. Fluids*, **27**, 2676 (1984).

[43] A. BHATTACHARJEE and E. HAMEIRI, *Phys. Fluids*, **31**, 1153 (1988).

[44] R. W. MOSES and K. F. SCHOENBERG, *Bull. Am. Phys. Soc.*, **34**, 2105 (1989).

[45] J. N. DiMARCO, these proceedings.

[46] R. W. MOSES, in *Proceedings of the Int. Workshop on Engineering Design of Next Step RFP devices*, Los Alamos National Laboratory Report LA-11139-C, 343 (1987).

[47] J. N. DOWNING, *Proc. 12th IEEE Symposium on Fusion Engineering*, 104 (1987).

END

DATE FILMED

11/29/90